Highlights

Finding Mechanisms of Exceptional Mobility using Numerical Algebraic Geometry

Charles W. Wampler, Mark Plecnik

- Sharply defines exceptional mobility using ideas from algebraic geometry.
- Applies the concept to both overconstrained mechanisms and robot self-motion.
- Explains a geometric construction for finding such mechanisms.
- Shows that numerical algebraic geometry can compute this construction.
- Illustrates graphically the mathematical concepts on several examples.

Finding Mechanisms of Exceptional Mobility using Numerical Algebraic Geometry

Charles W. Wampler[a,1], Mark Plecnik[a,2]

[a] *University of Notre Dame, Notre Dame, 46556, IN, USA*
cwample1@nd.edu, plecnikmark@nd.edu

Abstract

Mechanisms of exceptional mobility, including both overconstrained mechanisms and robots with self-motion, move with more degrees of freedom than predicted by the Grübler-Kutzbach formulas. Although a number of such cases are known, it is difficult to find new examples. This article explains a geometric formulation, called a fiber product, that facilitates finding exceptional mechanisms using tools from numerical algebraic geometry. The purpose of this article is to specialize the mathematical theory developed in [1] to the realm of kinematics and to present simple planar, spherical, and spatial examples that illustrate basic concepts. Although the formulation is general, its application to more complicated mechanisms will require the development of more refined solution techniques that exploit the symmetry inherent in fiber products.

Keywords: kinematics, overconstrained mechanism, robot self-motion, exceptional mobility, polynomial continuation, numerical algebraic geometry

1. Introduction

Mechanisms of exceptional mobility move with more degrees of freedom (DOFs) than the more general mechanisms in the same family. This includes both "overconstrained mechanisms" and cases of robot self-motion. The concept of an overconstrained mechanism derives from the fact that

[1]Supported in part by the Huisking Foundation, Inc. Collegiate Research Professorship.
[2]Supported in part by NSF Grant No. CMMI-2144732

when one writes loop equations in a straightforward manner, there appear to be at least as many constraint equations as joint variables, so that one might expect only isolated solutions or none at all. Accordingly, the Grübler-Kutzbach and related formulas predict a mobility of zero or less, implying that the mechanism is an immobile structure or that it cannot be assembled. Yet, exceptional mechanisms do move because their loop equations are not independent. The more general phenomenon of exceptional mobility includes mechanisms whose mobility as predicted by Grübler-Kutzbach formulas is positive—so strictly speaking they are not overconstrained—but they move with even more degrees of freedom than expected. In any of these cases, to be exceptional, the geometric parameters of the links of the mechanism—link lengths, link twists, and so on—must satisfy extra conditions. Moreover, an exceptional family of mechanisms can contain subsets of mechanisms that move with greater mobility than a general member, that is, there may be exceptions within exceptions, forming a stratification of the original parent family into sequentially smaller sets of increasing mobility.

Our treatment of exceptional mobility also applies to problems of robot self-motion. Sometimes these directly correspond to an equivalent overconstrained mechanism. For example, the conditions wherein a 6R serial-link robot can move its joints while holding its end-effector fixed in space corresponds to a mobile 6R loop. Conversely, under certain conditions, a 6SPU parallel-link robot (commonly called a Stewart-Gough platform) can move even though its leg-lengths are held constant, which makes it equivalent to a mobile 6SU platform. More generally, viewing a robot as an n-DOF device that relates configuration-space coordinates, such as joint angles, to operational space coordinates, such as end-effector location, an analyst may cast any problem wherein the robot retains positive mobility while holding n coordinates constant as a case of exceptional mobility. Furthermore, suppose we designate $m \leq n$ coordinates as parameters. If we hold those m parameters constant at general values, the robot will still have $n-m$ degrees of freedom. However, there may exist settings of the m parameters where the robot has more than $n-m$ freedoms of motion. In such configurations, the robot can be said to have exceptional mobility. Cases of this kind of exceptional mobility are similar to cases of mobility for overconstrained mechanisms except that now the set of parameters is expanded to include both link parameters and the m specially designated coordinates.

There is a misconception held by some that overconstrained mechanisms are useless because in practice, due to tolerances in manufacturing tech-

niques, one can never build a mechanism that exactly satisfies the algebraic conditions for mobility. This is thought to imply that either the mechanism will not move or that moving it will induce high internal forces that will cause the device to fail. This misconception persists because there is a nugget of truth behind it: a mechanism built near yet sufficiently far from the conditions for mobility will be a structure whose closure equations have an ill-conditioned Jacobian matrix, which implies that there exists a direction (or directions) of motion that are weakly constrained. All that is necessary for an overconstrained mechanism to move freely is that it is built accurately enough that elasticity and joint clearances can absorb small misalignments. After all, planar four-bars, the most commonly deployed class of mechanism, are overconstrained 4R spatial mechanisms. If misalignments are greater than the links and joints allow, then it is possible that applications of force or torques in certain directions will cause large internal forces to be generated. Even so, accommodation for relatively large departures from the ideal conditions can be designed into a mechanism, such as adding an elastic hinge or replacing an R joint with an S joint having a small range of travel; compliant mechanisms often rely on this phenomenon. Setting certain motion variables to be fixed, as is done when analyzing robot self-motions, imposes geometric constraints not enforced by physical links. As such, under non-ideal conditions, this "fixed" geometry will deviate slightly in a real robot, but the result is still a self-motion by practical measures.

For conciseness, in this paper, we will refer to mechanisms of exceptional mobility as simply "exceptional mechanisms," even though other types of exceptional behavior could be considered, such as exceptional multiplicity. For example, a general 6R spatial loop assembles in at most 16 isolated structures, each one a nonsingular solution of the loop equations. A special 6R spatial loop that assembles in a singular configuration, that is, in an isolated solution with multiplicity at least 2, will be "shaky," tending in practice to allow small displacements but not a full motion curve. Such a mechanism has exceptional multiplicity but not exceptional mobility, although one might say that the mechanism has exceptional infinitesimal mobility. In this paper, we consider only cases with true exceptional mobility, such as a 6R spatial loop that has a full motion curve.

Exceptions occur when the parameters of a mechanism, such as its link lengths, twists, and offsets, obey certain interrelationships. A familiar example is that a 4R spatial loop has Grübler-Kutzbach mobility of -2, and yet there exist three exceptional cases that move with 1-DOF, these being the

planar, spherical, and Bennett four-bars [2]. Grübler-Kutzbach formulas can easily be corrected for planar and spherical mechanisms by changing the ambient displacement space, and by adopting the approach introduced by Hervé [3], one may correctly calculate mobility for mechanisms with sub-chains that move in different displacement groups. Even so, examples such as the Bennett four-bars elude the grasp of these formalisms and require more individualized analyses. Because their existence seems so peculiar, such mechanisms have sometimes been classified as "paradoxical" [4].

Although a thorough review of the known exceptional mechanisms is beyond the scope of this article, a few examples are illustrative. For single-loop four-bar mechanisms, Bennett found his eponymous linkage in 1903 [2], Delassus showed in 1922 that for rotational joints, the only types of moveable 4R loops are planar, spherical, and Bennett [5], and Waldron expanded the analysis to include the other lower-pair joints [6]. Exceptional five- and six-bar spatial loops also exist [7, 8, 9, 10, 11], with further analysis in [12] and a full classification of 5R loops in [13]. Planar cognate linkages, wherein two different linkages reproduce the same motion, can be used to construct overconstrained linkages by connecting them. Accordingly, two Roberts four-bar cognates [14] can be connected to form a moveable seven-bar linkage (see Figure 1), and eleven-bar overconstrained linkages can be constructed with the six-bar curve cognates cataloged by Dijksman [15]. In that vein, the general approach in [16] for constructing planar cognates can generate a multitude of examples. Another subject of study has been Stewart-Gough platforms with self-motion [17, 18, 19, 20].

This article concerns going beyond the task of calculating the true mobility of a given mechanism to the harder task of characterizing what exceptions exist within a given parameterized family of mechanisms. The predominant approach in the kinematics community is to reduce the loop-closure conditions for a structure, such as a general 6R spatial loop, to a univariate polynomial and then study the conditions placed on the linkage parameters for the coefficients to vanish [12], sometimes simplifying the problem by first considering only the rotational part, $SO(3)$, of $SE(3) = \mathbb{R}^3 \times SO(3)$ [21]. Using computational symbolic algebra, one may reformulate this principle as the vanishing of the initial forms of a Gröbner basis [22, 23, 24] or a Dixon determinant [25]. In this paper, we explain a more geometric approach, amenable to the tools of numerical algebraic geometry, drawing heavily on the developments reported in [1].

Numerical algebraic geometry comprises a family of techniques for solving

systems of polynomial equations, including systems with positive-dimensional solution sets and multiple components. To find exceptional mechanisms with these tools, the key step is to use the loop closure equations of a parent family to form a new system in which the exceptions, originally hidden inside the parent family, are promoted to become their own irreducible solution components. These then stand out independent of their parents so that numerical algebraic geometry can find them. In principle, the formulation we present can be applied iteratively to find exceptions within exceptions forming a tree where each child moves with more degrees of freedom than its parent.

The purpose of this article is to translate the abstract developments in [1] to the specific case of kinematics. This begins with more careful definitions of mobility (Section 3) and exceptional mechanisms (Section 4), where the definition of exceptionality is not based on noting where mobility formulas fail but rather is given geometrically. By casting the problem as a geometric one, we will see how that geometry can be probed by slicing (Section 5) to find the exceptional sets. A key concept is a mathematical construction called a *fiber product*, which we explain geometrically as the intersection of projections. With this concept clarified, in Section 6, we describe the tools from numerical algebraic geometry that can find families of exceptional mechanisms given only the loop closure equations for the parent family. In Section 7, the approach is illustrated on several simple examples. Section 8 discusses how mobility may differ between real and complex sets. We end with a discussion (Section 9) of the further developments that will be needed to bring more significant cases within practical computational limits.

2. Notation

We use the following definitions and notations. The more technical terms among these are discussed further in subsequent sections.

$\mathbb{R}^n$, $\mathbb{C}^n$	Real and complex n-dimensional Cartesian spaces
$\theta \in \Theta$	Variables θ that define *configuration space* Θ, usually associated with a mechanism's motion.
$p \in P$	Parameters p belong to *parameter space* P, which consists of the mechanism's design parameters and possibly also including a subset of a robot's joint variables or operational space coordinates.

$f(\theta; p)$ A polynomial system with variables θ and parameters p.

$V(g(x))$ The solution set of polynomial system $g(x) : X \to Y$. That is, $V(g) = \{x \in X \mid g(x) = 0\}$. $V(g)$ consists of one or several irreducible components, i.e. algebraic subsets that cannot be decomposed into a finite number of proper algebraic subsets.

$V(f(\theta; p))$ The algebraic subset of $\Theta \times P$ that consists of an entire family of mechanisms and their motions.

$V(f(\theta; p^*))$ The motion of a single mechanism $p^* \in P$.

A Some algebraic set, for example, an irreducible component within $\Theta \times P$ of $V(f(\theta; p))$.

$\dim_z A$ The local dimension of A at point z. If z lies at the intersection of several components of different dimension, $\dim_z A$ is the largest of these.

π A projection map $\pi : V(f) \to P$, that strips off the variables: $(\theta; p) \mapsto (p)$. π^{-1} recovers the motion of the mechanism having parameters p, hence $\pi^{-1}(p^*) = V(f(\theta; p^*))$, also called the *fiber* of $V(f)$ over p^*.

$\dim_{(\theta^*, p^*)} \pi^{-1}(p^*)$ The local dimension of a mechanism with parameters p^* for a motion that includes θ^*. This is the *mobility* of the mechanism in that assembly configuration.

$\overline{A}$ When A is a constructible algebraic set (the result of a finite number of Boolean operations involving algebraic sets), $\overline{A}$ is the closure of A in complex space, which makes $\overline{A}$ an algebraic set. This fills in "missing" points, for example, the projection of $V(xy - 1)$ onto x is all of the x-axis except $x = 0$. Closure fills in this point. Projection followed by closure is the geometric equivalent of algebraic elimination.

$D_{\mathfrak{m}}$ The "$\mathfrak{m}$-mobility set", an algebraic set within $\Theta \times P$ comprised of the closure of the constructible set of all mechanisms and their motion components that have mobility $\mathfrak{m}$. *We wish to study the sets $D_{\mathfrak{m}}$ as $\mathfrak{m}$ varies.*

$\mathfrak{b}$ For irreducible set $A \in V(f(\theta;p))$, $\mathfrak{b} = \dim(\pi(A))$ is the *base* dimension of A. For a general point $(\theta^*;p^*) \in A$ with mobility $\mathfrak{m}$, $\mathfrak{m} + \mathfrak{b} = \dim A$.

$F_k(\theta_1,\ldots,\theta_k;p)$ A polynomial system $F_k : \Theta^k \times P \to \mathbb{C}^{kn}$, constructed from k copies of $f(\theta;p)$, k copies of the configuration space Θ, and a single copy of parameter space P. $F_k(\theta_1,\ldots,\theta_k;p) = \{f(\theta_1;p),\ldots,f(\theta_k;p)\}$, is the k-th *fiber product system.*

$\mathcal{L}_k(x)$ A system of k linearly independent linear polynomials in x, these being of the form $\mathcal{L}_k(x) = Cx+d$ where coefficient matrix C and coefficient vector d are populated with random entries. For shorthand, when more than one such system appears in the same expression, we mean that each instance has its own coefficients selected independently of the others.

$G_k^{(\mathfrak{b},\mathfrak{m})}(\theta_1,\ldots,\theta_k;p)$ A polynomial system $G_k^{(\mathfrak{b},\mathfrak{m})} : \Theta^k \times P \to \mathbb{C}^{k(n+\mathfrak{m})+\mathfrak{b}}$, constructed from k copies of $f(\theta_j;p)$, k linear systems $\mathcal{L}_\mathfrak{m}(\theta_j)$, and a single linear system $\mathcal{L}_\mathfrak{b}(p)$. $G_k^{(\mathfrak{b},\mathfrak{m})}$ is called a k-th *fiber product sliced system.*

$\Pi^k A$ The k-th fiber product of A with itself. For $A \in V(f(\theta;p))$, $\Pi^k A$ is an algebraic subset of $V(F_k)$. Its projection onto parameter space is $\pi_k\big(\Pi^k A\big) \subset P$.

3. Definition of Mechanism Mobility

Before searching for mechanisms of exceptional mobility, we must sharply define mobility.

Although the basic ideas could be generalized, we confine our discussion to linkages having algebraic joint types, these being rotational (R), prismatic (P), planar (E), spherical (S), and cylindrical (C), but excluding helical (H). Given only a list of links and how they are connected by joints, one may write loop closure equations in the form $f(\theta;p) = 0$, where θ is an array of joint variables, p is an array of link parameters, and f is a system of polynomial equations. For example, one might adopt the Denavit-Hartenberg (DH) formalism to write equations for the closure of the ℓ-th loop involving

n links connected by rotational joints in the form

$$f_\ell(\theta; p) = T_1(\theta_1; d_1, a_1, \alpha_1) \cdots T_n(\theta_n; d_n, a_n, \alpha_n) - I = 0,$$
$$\theta = (\theta_1, \ldots, \theta_n), \quad p = (d_1, a_1, \alpha_1, \ldots, d_n, a_n, \alpha_n),$$

where θ_i is the rotation angle of the i-th joint, and (d_i, a_i, α_i) are the length, offset, and twist of the i-th link. Then, an m-loop mechanism is modeled as

$$f(\theta; p) = \{f_1(\theta; p), \ldots, f_m(\theta; p)\} = 0,$$

where arrays θ and p are expanded to include all the links and joints in the multi-loop mechanism, and where some links and joints typically appear in several loops. We note that in questions of robot self-motion, the parameters p may include the operational space coordinates of the robot.

In the standard DH formalism, these equations are trigonometric, not algebraic, but they can be converted to polynomials by replacing θ_i with the pair $(c_i, s_i) = (\cos\theta_i, \sin\theta_i)$ and appending the polynomial $c_i^2 + s_i^2 - 1$ to the system. (A tangent-half-angle transformation could be used instead.) A similar transformation applies to the twist angles, α_i. For this paper, we do not care what formalism is used to generate the equations, we only care that they are algebraic. In fact, the DH formalism is often not the most advantageous way to present equations for numerical computations.

Using the notation of Section 2, the algebraic set $V(f) \subset \Theta \times P$ consists of all members of a mechanism family along with their solution sets. For a given mechanism, that is, for a point $p^* \in P$, the solution set $V(f(\theta; p^*)$ is empty if the mechanism cannot be assembled; it is zero-dimensional if the mechanism can be assembled but only as a rigid structure (or it can be assembled in one of several such structures); it is one-dimensional if the mechanism moves along a 1DOF motion curve; and so on for higher dimensions. For brevity, we may refer to $V(f(\theta; p^*))$ as the "motion" of mechanism p^* even when it assembles in a zero-dimensional rigid structure rather than a positive-dimensional motion. The motion can always be decomposed into a union of irreducible algebraic sets, which we will call "irreducible motions." When a mechanism has more than one irreducible motion, it is possible for two of them to meet, at which point the mechanism can transfer from one to the other, as in the example in [26]. If two irreducible motions of different dimensions meet, the mechanism can be called a *kinematotropic* or *variable-DOF* linkage [27, 28, 29], also related to *metamorphic* mechanisms [30].

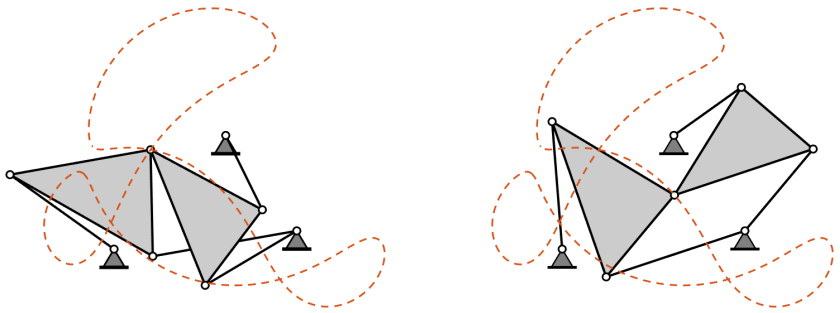

Figure 1: A seven-bar linkage. In assembly configuration (a), the linkage has mobility 0 (rigid structure), whereas in assembly configuration (b), it moves with mobility 1 along the dashed coupler curve. Two mobility 0 solutions occur at each of the three nodes of the coupler curve.

We wish to equate the *mobility* of a mechanism to the dimension of its solution set. But since the entire motion can have several irreducible motions of different dimensions, it is more proper to speak of the mobility of the individual irreducible motions rather than the mobility of the mechanism. An example is the mechanism shown in Figure 1 formed by connecting the coupler points of two four-bars that are Roberts cognates. The resulting seven-bar linkage has seven irreducible motions. In one, the linkage moves with 1DOF along the shared coupler curve of the four-bars. But since the coupler curve has a real self-intersection point, the two four-bars can also be connected in such a manner that the resulting seven-bar is a rigid structure, because the component four-bars are positioned on different segments of the coupler curve. With two such structures occurring at each of three crossing points of the coupler curve, the seven-bar mechanism can be assembled as either a mobility 1 linkage or as any one of six different mobility 0 structures.

Because a mechanism can have irreducible motions of different mobility, it is more proper to equate mobility to the *local dimension* at a point $(\theta^*; p^*)$, where θ^* specifies an assembly configuration and, therefore, generally identifies a specific irreducible motion. If θ^* is a point where two or more irreducible motions intersect, the local dimension, and by our definition the mobility, is the largest dimension among those irreducibles.

So far we have used the term "dimension" relying on the reader's familiarity with that concept, but further investigation will be facilitated by defining it more carefully. We start at dimension zero, where for $g : \mathbb{C}^n \to \mathbb{C}^m$,

a solution point $x \in V(g)$ is *isolated* if it is the center of an open ball, $\{z \in \mathbb{C}^n \mid ||z - x|| < r\}, r > 0$, that contains no other solution. This can be checked by evaluating g and its partial derivatives at x [31]. If the Jacobian matrix of first partial derivatives of g evaluated at x has full column rank, then x is an isolated nonsingular solution, while higher-order derivatives are needed to confirm that a singular solution is isolated. If x is not isolated, we can try to make it so by appending linear equations to $g(z)$ of the form $w^T(z - x) = 0$, where w is a general vector in $\mathbb{C}^n$. At worst g is the identically zero polynomial, in which case appending n general linear equations isolates x. This implies that there exists a smallest integer d, $0 \leq d \leq n$, such that appending d of these linear equations isolates x. Then, d is the local dimension of $V(g)$ at x, written $d = \dim_x V(g)$. (If x has multiplicity 1, then the associated vectors $w_1, \ldots, w_d$ form a basis for a local coordinate chart on $V(g)$ in the neighborhood of x. This comports with the notion that dimension is the number of coordinates needed to build a local chart at x.) By this definition, one sees that if x happens to lie at the intersection of several components, the local dimension at x is the largest dimension among these components.

Numerical algebraic geometry depends on the foregoing definition of dimension. Given that we can build homotopies guaranteed to find all isolated solutions of any polynomial system, d-dimensional solution components for $d > 0$ are witnessed by finding the isolated solutions of system $\{g(z), L(z)\}$, where $L(z)$ is a system of d general linear equations. A structure containing three elements—system g, slicing system L, and the witness point set $V(g, L)$—is called a *witness set* for the d-dimensional component of $V(g)$. These can be further decomposed into *irreducible components*. A *numerical irreducible decomposition* algorithm tries all possible dimensions and compiles a list of witness sets, one for each irreducible component. A basic text describing the main algorithms of the field is [32], which also documents `Bertini` [33], one of the leading software implementations. Other software implementations include `HomotopyContinuation.jl` [34], `NAG4M2` [35], and `PHCpack` [36].

An irreducible decomposition of the loop equations $f(\theta; p^*)$ gives the dimension and degree of each irreducible motion of the mechanism with parameters p^*; the mobility of each irreducible motion is its dimension. For a family of mechanisms, we may find the general behavior by choosing a random example for p^*. Solving over the complex numbers leverages the algebraic closure of the complex number field to eliminate any concern that

we will miss seeing an irreducible motion; we can even choose the test point, p^*, to be non-real. The number of irreducible motions and their mobilities in complex space will be the same for almost all members of the family. However, we must keep in mind that although a degree n polynomial always has n roots over the complex number field, the number of real roots varies as the coefficients vary. In the same way, while irreducible motions always persist in complex space, their intersection with the reals can disappear and reappear as parameters are varied. We defer a more detailed consideration of this to Section 8.

4. Definition of Exceptional Mechanisms

As we look across a whole family of mechanisms, that is, as we let p^* vary across the parameter space P, the decomposition of $V(f(\theta; p^*))$ into irreducible motions has the same structure for almost all $p^* \in P$, meaning that there are the same number of irreducible motions of the same dimension and degree. However, there may exist subsets of P where the decomposition into irreducible motions has a different structure, and in particular, there may exist points where there exists an irreducible motion of a dimension larger than occurs in its general neighborhood. Such subsets are *exceptional mechanisms*.

While irreducible decomposition provides a complete mobility analysis of a given mechanism, be it general or exceptional, it does not tell us where to find exceptions. That job requires us to treat the parameters as variables and build a system of polynomials whose irreducible components identify with exceptional mechanisms. We will first illustrate basic concepts using the systems shown in Figure 2. Although these are not mechanisms, they are of the form $f(\theta; p)$ and have easily understood solution sets. After discussing the basic concepts, we will illustrate them again on simple mechanisms.

We begin with a careful definition of exceptionality, which is facilitated by introducing the concepts of projections and their fibers. Given a mechanism in an assembly configuration, $(\theta; p) \in V(f(\theta; p))$, we define the projection $\pi : V(f) \to P$ by the map $(\theta; p) \mapsto (p)$. So π just strips away the motion and gives us the mechanism as described by its parameters. (This may seem rather trivial, but it gives a precise way of writing basic principles.) The inverse of π, i.e., $\pi^{-1} : P \to V(f)$ reconstitutes the motion, and $\pi^{-1}(p^*)$ is called the "fiber over p^*." For point $p^* \in P$, the fiber $\pi^{-1}(p^*)$ is empty if the mechanism p^* cannot be assembled, while for $(\theta^*; p^*) \in V(f)$ the mechanism

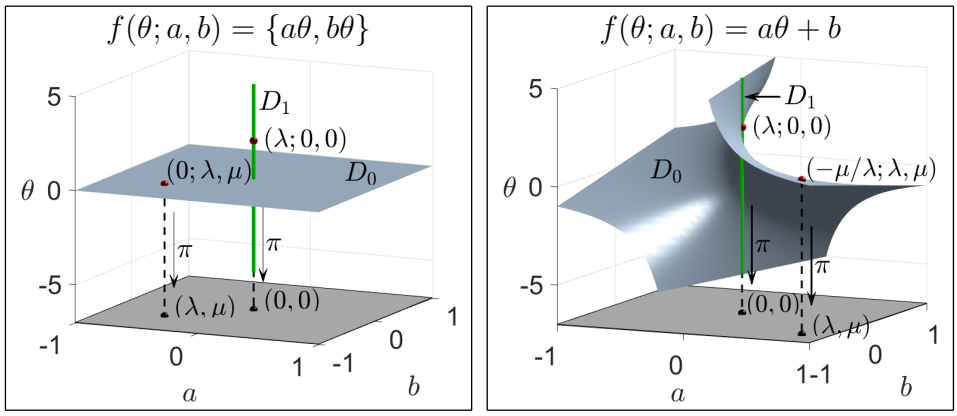

Figure 2: Two examples of a parameterized polynomial system $f(\theta; a, b)$ which has a unique point $(a^*, b^*) \in \mathbb{C}^2$ where $V(f(\theta; a^*, b^*))$ has exceptional dimension. In both cases, the 1-dimensional exceptional set is the highlighted line $D_1 = \{(\lambda; 0, 0), \lambda \in \mathbb{C}\}$. Dots on D_0 and D_1 are a mechanism in an assembly configuration, each of which π projects to a corresponding point in the parameter plane below. (a) Exceptional set D_1 arises as an irreducible component of $V(f)$. (b) Exceptional set D_1 is embedded inside D_0.

satisfies the loop equations, so $\pi^{-1}(\pi(\theta^*; p^*))$ is the entire motion of the mechanism and $\dim_{(\theta^*;p^*)} \pi^{-1}(\pi(\theta^*; p^*))$ is the dimension (and therefore the mobility) of the motion component of mechanism p^* that $(\theta^*; p^*)$ belongs to. We can scan across all mechanisms in the family and, for each of these, pick out the irreducible motions of a given mobility, $\mathfrak{m}$. The union of all these mechanisms and their mobility $\mathfrak{m}$ motions form the algebraic set

$$D_{\mathfrak{m}} \stackrel{\text{def}}{=} \overline{\{(\theta; p) \in V(f) \mid \dim_{(\theta;p)} \pi^{-1}(\pi(\theta; p)) = \mathfrak{m}\}}. \tag{1}$$

The over-bar means closure in complex space, which fills in "missing" points to make the set complete. Let us call $D_{\mathfrak{m}}$ the "$\mathfrak{m}$-mobility set" of the family of mechanisms.

To clarify, the introduction of the projection and its inverse in definition (1) is necessary to associate mobility with the dimension of motion. Mobility is not the local dimension $\dim_{(\theta^*;p^*)} V(f(\theta; p))$, because that dimension includes the freedom to move p in parameter space. Instead, mobility is the dimension of an irreducible motion in the fiber over a specific mechanism p^*, and the $\mathfrak{m}$-mobility set $D_{\mathfrak{m}}$ is the union of all $\mathfrak{m}$-dimensional motions as p^* varies over P.

This concept is illustrated in Figure 2 for two systems: $f(\theta; a, b) = \{a\theta, b\theta\}$ and $f(\theta; a, b) = a\theta + b$. (For purposes of illustration, we are not

using actual loop equations here.) Two points in $V(f)$ are marked, one with general parameters and one with special parameters. For each of the systems, if (a, b) have general values, then θ is determined uniquely. One of the two points marked in each figure is of this type, so it belongs to set D_0. The second point in each case has the special parameter values $(a, b) = (0, 0)$, which leaves θ free to vary along a 1-dimensional motion. We see that in each case, D_0 is a 2-dimensional set that covers all of parameter space, whereas D_1 is a 1-dimensional line over $(a, b) = (0, 0)$. Set closure just means that both D_0 and D_1 contain the points where they intersect.

For any mechanism family $f(\theta; p)$, there is a smallest mobility $\mathfrak{m}_{\min}$ such that $D_{\mathfrak{m}_{\min}} \neq \emptyset$. If there exists $D_{\mathfrak{m}} \neq \emptyset$ for $\mathfrak{m} > \mathfrak{m}_{\min}$, we may say that members of $D_{\mathfrak{m}}$ have exceptional mobility. In some cases, like Figure 2(a), D_0 and D_1 are separate irreducible components, but in other cases, like Figure 2(b), D_1 is embedded inside of D_0. For families with more parameters, there may be more than two levels of exceptions, and so there also may be exceptions embedded within exceptions, etc.

4.1. Base and Fiber Dimension

To review, point $(\theta^*; p^*) \in V(f)$ is a mechanism in an assembly configuration. Then, $\pi(\theta^*; p^*) = p^*$ is just the mechanism, and $\pi^{-1}(p^*) = V(f(\theta; p), p - p^*)$ is that mechanism's entire motion, which may consist of several irreducible motions, at least one of which includes the assembly configuration θ^*. Finally, $D_{\mathfrak{m}}$ is the union of all the irreducible motions of mobility $\mathfrak{m}$ taken across all the mechanisms in the family where those motions exist.

Each set $D_{\mathfrak{m}}$ is an algebraic set, so it can be decomposed into irreducible components. Suppose A is one of these irreducible components, and $(\theta^*; p^*)$ is a generic point of A. Then, $A \cap V(p - p^*)$ is the motion of mechanism p^* belonging to A, which by the definition of $D_{\mathfrak{m}}$ has mobility $\mathfrak{m}$. In the parlance of algebraic geometry, $A \cap V(p - p^*)$ is the fiber over p^* passing through $(\theta^*; p^*)$, and $\mathfrak{m}$ is its *fiber dimension*. Meanwhile, $\overline{\pi(A)}$ is the subset of mechanisms that all have this same irreducible motion. We may call $\dim \overline{\pi(A)} = \mathfrak{b}$ the *base dimension* of A. Combining the two measures, we say that A has *bi-dimension* $(\mathfrak{b}, \mathfrak{m})$. Since every general point in A has fiber dimension $\mathfrak{m}$, it is clear that these dimensions add, that is,

$$\dim A = \mathfrak{b} + \mathfrak{m}. \tag{2}$$

In the examples of Figure 2, each D_0 has base dimension $\mathfrak{b} = 2$ and mobility $\mathfrak{m} = 0$, for a total dimension of 2, while each D_1 has base dimension $\mathfrak{b} = 0$ and mobility $mob = 1$, for a total dimension of 1. (In [1], the letters (b, h) are used instead of $(\mathfrak{b}, \mathfrak{m})$. We use $\mathfrak{m}$ here to emphasize that in the current context it is equivalent to mobility.)

Suppose that A' is an irreducible component of $D_{\mathfrak{m}'}$ with base dimension $\mathfrak{b}'$. If A' is a proper subset of A, $A' \subsetneq A$, then $\dim A' < \dim A$. Because mobility is an algebraic property, the principle of upper semicontinuity applies, and thus $\mathfrak{m}' \geq \mathfrak{m}$, and in fact, $\mathfrak{m}' > \mathfrak{m}$ because that is the property that distinguishes A' from A. Altogether, using (2), we have that the possible dimensions for A' are the integers in the triangle given by the following three inequalities

$$\mathfrak{b}' + \mathfrak{m}' \leq \mathfrak{b} + \mathfrak{m} - 1, \quad \mathfrak{b}' \geq 0, \quad \mathfrak{m}' \geq \mathfrak{m} + 1. \tag{3}$$

In particular, in Figure 2(b), we see that since D_0 has base dimension $\mathfrak{b} = 2$, the only possible size of an exceptional set contained within it is $(\mathfrak{b}', \mathfrak{m}') = (0, 1)$, which is the case of D_1 as shown. In fact, the above inequalities imply that for any A' embedded inside A, the base dimensions obey

$$\mathfrak{b}' \leq \mathfrak{b} - 2. \tag{4}$$

Although it does not happen for the examples in Figure 2, in general it would be possible for a set with bi-dimension $(1, 1)$ to exist, but since its total dimension of 2 would be the same as the dimension of D_0, it could not be contained inside D_0. Instead, it would be a separate component of D_1.

5. Finding Witness Points by Structured Slicing

If an irreducible component of $D_{\mathfrak{m}}$ is also an irreducible component of $V(f)$, then we can find it by performing an irreducible decomposition of $V(f)$. Recall from Section 3 that the standard way of doing that is to append d linear equations to system f and solve that augmented system to find witness points on d-dimensional components of $V(f)$.

For conciseness, let's denote by $\mathcal{L}_k(x)$ a set of k general linear equations in the variables of x. So if $x \in \mathbb{C}^n$, then $\mathcal{L}_k(x) = Cx + d$, where C is a $k \times n$ matrix, d is $k \times 1$, and the entries of C and d are chosen at random. Geometrically, since a random matrix has full rank (with probability 1), the solution set $V(\mathcal{L}_k(x))$ is an affine linear space of dimension $n-k$. In practice,

the entries in C, d will be complex numbers of approximately magnitude 1, picked using a random number generator with as many digits as the numerical precision used in computations. For illustration in this article, we use real numbers with just a few digits.

For an irreducible component, say A, of $D_{\mathfrak{m}}$ with base dimension $\mathfrak{b}$ and mobility $\mathfrak{m}$, we know that intersecting A with the solution sets of $\mathfrak{m}$ linear equations in just θ, say system $\mathcal{L}_{\mathfrak{m}}(\theta)$ and $\mathfrak{b}$ linear equations in just p, say $\mathcal{L}_{\mathfrak{b}}(p)$, will result in isolated points: $\dim\big(A \cap V(\mathcal{L}_{\mathfrak{m}}(\theta)) \cap V(\mathcal{L}_{\mathfrak{b}}(p))\big) = 0$. If A is also an irreducible component of $V(f)$, then these points are also isolated points in $V\big(f(\theta; p), \mathcal{L}_{\mathfrak{m}}(\theta), \mathcal{L}_{\mathfrak{b}}(p)\big)$. Because we target the bi-dimension $(\mathfrak{b}, \mathfrak{m})$ directly, this is a more focused way of finding A than targeting its total dimension using $V\big(f(\theta; p), \mathcal{L}_{\mathfrak{b}+\mathfrak{m}}(\theta; p)\big)$. Similar to the way a standard irreducible decomposition algorithm steps through all possible dimensions, an algorithm can step through all possible combinations of $(\mathfrak{b}, \mathfrak{m})$ to find all sets $D_{\mathfrak{m}}$ that are irreducible components of $V(f)$.

As an example, consider again Figure 2(a), where both D_0 and D_1 are irreducible components of $V(a\theta, b\theta)$. We find D_0 by solving a system of the form $\{a\theta, b\theta, \mathcal{L}_2(a, b)\}$. Since $\mathcal{L}_2(a, b)$ picks out a generic, and therefore nonzero, point in parameter space, say $(a, b) = (a^*, b^*)$, we obtain $(\theta; a, b) = (0; a^*, b^*)$ as a witness point for D_0. We find D_1 by solving $\{a\theta, b\theta, \mathcal{L}_1(\theta)\}$, that is, by solving $\{a\theta, b\theta, \theta - \theta^*\}$ where θ^* is just a generic value nonzero value. Consequently, we obtain $(\theta^*; 0, 0)$ as a witness point. Notice that a search for a set of bi-dimension $(\mathfrak{b}, \mathfrak{m}) = (1, 1)$ will come up empty.

The system $f = a\theta + b$ illustrated in Figure 2(b) presents a different situation, because D_1 is embedded inside D_0. Searching for a set of bi-dimension $(\mathfrak{b}, \mathfrak{m}) = (2, 0)$ works as before to give a witness point of the form $(-b^*/a^*; a^*, b^*)$, where (a^*, b^*) is a generic point in parameter space. But a slice searching for solutions of bi-dimension $(\mathfrak{b}, \mathfrak{m}) = (0, 1)$ would solve the system $\{a\theta + b, \mathcal{L}_1(\theta)\}$, whose solution is just the line $\{\theta = \theta^*, a\theta^* + b = 0\}$ for a generic value of θ^*. That line intersects D_1 in a single point, but the system $\{a\theta + b, \mathcal{L}_1(\theta)\}$ does not single it out. In that sense, D_1 is "hidden" inside D_0. We need to impose more conditions to distinguish D_1 from D_0, and this will always be the case for embedded exceptional sets.

6. Finding Embedded Exceptional Sets

When an exceptional set, say A', is embedded inside another irreducible component, say A, of $V(f)$, a single slice of $V(f)$ doesn't isolate A'. We need

to form a new system that promotes A' to irreducibility so that slicing will isolate points on it. Fortunately, the theory in [1] tells us a way to do so: use a so-called fiber product formulation. In place of $f(\theta; p) : \Theta \times P \to \mathbb{C}^n$, we form the "doubled-up" system

$$F_2 : \Theta \times \Theta \times P \to \mathbb{C}^{2n}, \qquad F_2(\theta_1, \theta_2; p) = \{f(\theta_1; p), f(\theta_2; p)\}. \tag{5}$$

In fact, in some cases, we will need to go further to use a k-th fiber product system:

$$F_k : \Theta^k \times P \to \mathbb{C}^{kn}, \qquad F_k(\theta_1, \ldots, \theta_k; p) = \{f(\theta_1; p), \ldots, f(\theta_k; p)\}. \tag{6}$$

[In this notation, $F_1(\theta_1; p) \equiv f(\theta; p)$.]

On the face of it, (5) doesn't seem like it accomplishes much, but consider what happens in the case of Figure 2(b) when we slice $V(F_2)$ to find sets of bi-dimension $(\mathfrak{b}, \mathfrak{m})$. We now have two copies of configuration space, and so we need to slice both of these with $\mathfrak{m}$ general linear equations. Consequently, to find D_1, which has $(\mathfrak{b}, \mathfrak{m}) = (0, 1)$, we will solve the system

$$\{a\theta_1 + b,\ \theta_1 - \alpha,\ a\theta_2 + b,\ \theta_2 - \beta\}$$

where α and β are generic values. The result is shown in Figure 3 for $\alpha = 3, \beta = -2.5$, which has the solution $(\theta_1, \theta_2; a, b) = (3, -2.5; 0, 0)$. As the figure indicates, we may think of the fiber product as intersecting projections onto parameter space of slices of the surface, that is, computing $\pi\big(V(a\theta_1 + b, \theta_1 - 3)\big) \cap \pi\big(V(a\theta_2 + b, \theta_2 + 2.5)\big)$, to get the exceptional parameter point $(a, b) = (0, 0)$. It is a bit more than this though, because we also get two witness points on D_1, the points $(3; 0, 0)$ and $(-2.5; 0, 0)$.

The general idea, then, is to search for a set of bi-dimension $(\mathfrak{b}, \mathfrak{m})$ by slicing the fiber product system F_k, from (6), using a system $\mathcal{L}_\mathfrak{b}(p)$ to slice the base and an independent system $\mathcal{L}_\mathfrak{m}(\theta_i)$, $i = 1, \ldots, k$ in each fiber direction:

$$\begin{gathered} G_k^{(\mathfrak{b},\mathfrak{m})} : \Theta^k \times P \to \mathbb{C}^{k(n+\mathfrak{m})+\mathfrak{b}}, \\ G_k^{(\mathfrak{b},\mathfrak{m})}(\theta_1, \ldots, \theta_k; p) = \big\{\big[\big(f(\theta_i; p), \mathcal{L}_\mathfrak{m}(\theta_i)\big), i = 1, \ldots, k\big], \mathcal{L}_\mathfrak{b}(p)\big\}. \end{gathered} \tag{7}$$

It is to be understood that each appearance of a linear system $\mathcal{L}_j(x) = Cx + d$ is composed using a different choice of general C, d. The case illustrated in Figure 3 corresponds to solving $G_2^{(0,1)}$.

The fiber product is not just a trick that happens to work on the example $f = a\theta + b$; it works in general. This can be seen using the growth-rate argument from [1]. A bit of notation helps explain it. Note that the existence of

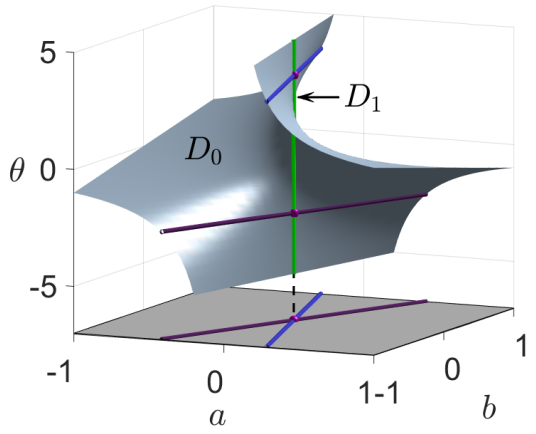

Figure 3: Surface $V(a\theta + b)$ sliced twice in a fiber product that reveals D_1.

a set $A \subset (V(f))$ of bi-dimension $(\mathfrak{b}, \mathfrak{m})$ implies that there is a corresponding set of multi-dimension

$$(\mathfrak{b}, \underbrace{\mathfrak{m}, \ldots, \mathfrak{m}}_{k \text{ times}})$$

in $V(F_k)$. Following [1], this descendant of A is denoted $\Pi^k A \subset \Theta^k \times P$, and its projection onto parameter space is $\pi_k\big(\Pi^k A\big) \subset P$.

The growth-rate argument notes that under the k-th fiber-product construction, set $A \subset V(F_1)$ with bi-dimension $(\mathfrak{b}, \mathfrak{m})$ and hence total dimension $\mathfrak{b} + \mathfrak{m}$, engenders a set $\Pi^k A \subset V(F_k))$ with total dimension $\mathfrak{b} + k\mathfrak{m}$. This means that if A' has bi-dimension $(\mathfrak{b}', \mathfrak{m}')$ and A has bi-dimension $(\mathfrak{b}, \mathfrak{m})$, with $\mathfrak{m}' > \mathfrak{m}$, then as k increases, A' gives birth to a set $\Pi^k A'$ whose total dimension grows faster than that of $\Pi^k A$. If A' is embedded in A as a solution of $V(f)$, at some point the total dimension of $\Pi^k A'$ will equal or exceed that of $\Pi^k A$, so it can no longer be wholly contained therein. The value of k where $\Pi^k A'$ becomes too big for $\Pi^k A$ to contain it occurs when

$$\mathfrak{b}' + k\mathfrak{m}' \geq \mathfrak{b} + k\mathfrak{m}, \quad \text{i.e.,} \quad k \geq (\mathfrak{b} - \mathfrak{b}')/(\mathfrak{m}' - \mathfrak{m}). \tag{8}$$

The worst case occurs when $\mathfrak{b}' = 0$ and $\mathfrak{m}' = \mathfrak{m} + 1$, so that we may need to deal with $V(F_{\mathfrak{b}})$. This is the case for $D_1 \subset D_0$ in Figure 3, where $\mathfrak{b}' = 0$, $\mathfrak{b} = 2$, and $k = 2$ suffices to find D_1.

One can think of this another way, using Figure 3 for inspiration. Each subsystem $\big(f(\theta_i; p), \mathcal{L}_{\mathfrak{m}}(\theta_i)\big)$ constrains p to a subset of P, and if a set of mobility $\mathfrak{m}$ exists, its projection on P will be in that set. Intersecting enough

of these projections will eventually cut out a set of dimension $\mathfrak{b}$ corresponding to a $\mathfrak{b}$-dimensional subfamily of mechanisms that all have at least one motion of mobility $\mathfrak{m}$. The linear system $\mathcal{L}_{\mathfrak{b}}(p)$ cuts out witness points on this set. While this can be a useful image for intuitive understanding, it is the growth argument that proves the procedure works and gives us a bound on the order, k, where irreducibility is achieved.

Although the growth argument gives a bound on k, this is just an upper bound; the first value of k that causes $\Pi^k A'$ to break free from $\Pi^k A$ may be less than the k given in (8). Another consideration is that it is possible that A' is embedded inside more than one set. Even so, there is still a smallest k where $\Pi^k A'$ is no longer contained in any set with lower mobility, at which point we may say that A' has been *promoted to irreducibility*.

7. Application to Exceptional Mechanisms

The systems in Figure 2 are not loop equations for a mechanism—they were chosen for easy visualization. In this section, we present several illustrative examples from kinematics.

7.1. 2R Robot Self-motion

Consider the $2R$ planar robot of Figure 4(a). As is well known, for general (x, y), this robot has two inverse kinematics solutions, but for the special case $\ell_1 = \ell_2$ with $(x, y) = (0, 0)$, it has a self-motion. These cases are illustrated in Figure 4(b,c), where angle θ_1 is plotted versus (x, y).

Let's consider two versions of the RR self-motion problem: (a) case $\ell_1 = \ell_2$, and (b) case ℓ_1, ℓ_2 general. In case (a), we know a self-motion exists, and we want to illustrate how the method finds it. In case (b), there is no self-motion in general, so we wish to discover the condition for one to exist. Case (a) is easy to illustrate graphically, while case (b) represents the kind of search one would undertake when trying to find a new kind of exceptional mechanism or self-motion.

Using a complex-plane formulation of planar kinematics, the loop equation for the RR robot is

$$\tilde{f}(\Theta_1, \Theta_2; \ell_1, \ell_2, x, y) = \ell_1 e^{i\Theta_1} + \ell_2 e^{i\Theta_2} - (x + iy) = 0. \tag{9}$$

We note that here, as in any study of self-motion, the operational space coordinates, (x, y), of the robot are considered parameters. We intend to search for cases where the robot moves while holding its endpoint in place.

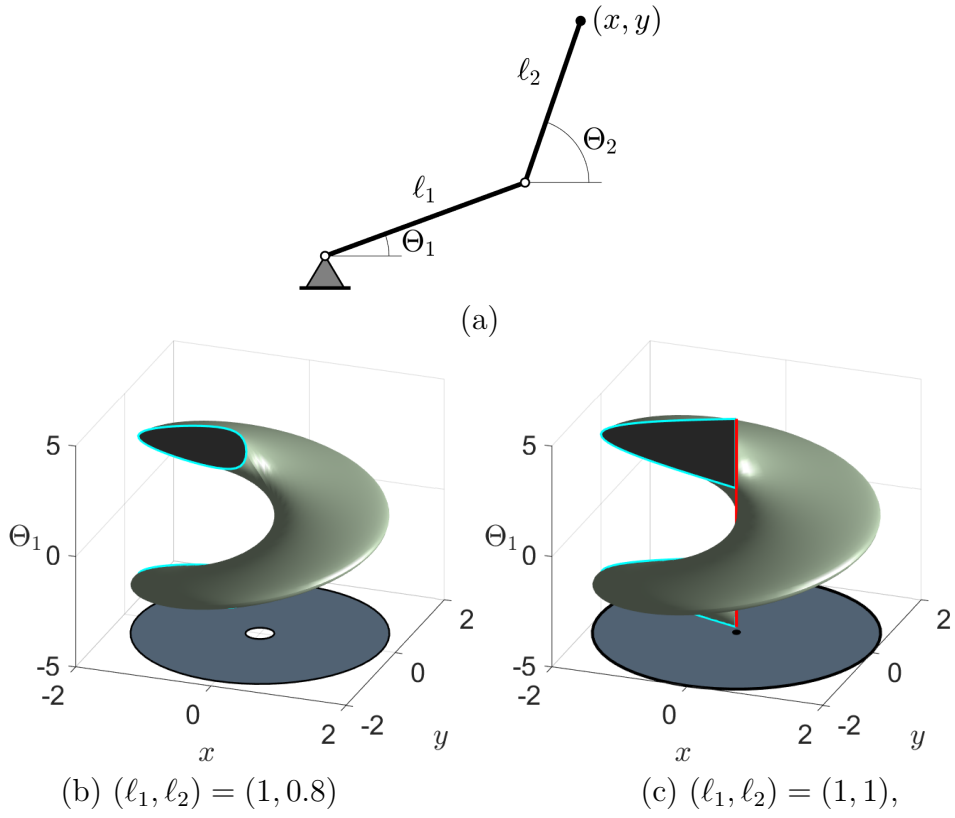

Figure 4: *RR* planar robot (a) and motion surfaces (b,c).

It is clear that the scale of the mechanism doesn't matter, so we may arbitrarily set $\ell_1 = 1$, taking note that this eliminates the degenerate case of $\ell_1 = 0$. To convert $\tilde{f}$ into a polynomial system, we switch to an isotropic formulation [37] in which for $j = 1, 2$, $\theta_j = e^{i\Theta_j}$ and $\bar{\theta}_j = e^{-i\Theta_j}$ and consider $\tilde{f}$ and its complex conjugate to form the system

$$f = \begin{Bmatrix} \theta_1 + \ell_2\theta_2 - (x + iy) \\ \bar{\theta}_1 + \ell_2\bar{\theta}_2 - (x - iy) \\ \theta_1\bar{\theta}_1 - 1 \\ \theta_2\bar{\theta}_2 - 1 \end{Bmatrix}. \tag{10}$$

When we slice $V(f)$ to find a self-motion with mobility $\mathfrak{m} = 1$, we assert that a self-motion where Θ_1 is stationary while Θ_2 moves is uninteresting, so a slice of the self-motion is equivalent to setting Θ_1 equal to a general value, say $\Theta_{1,j}$ in the j-th slice. (This move is not necessary for the method to succeed, as we could solve the problem using a general slice of the form $\mathcal{L}_1(\theta_1, \bar{\theta}_1, \theta_2, \bar{\theta}_2)$. We use the special slice $\Theta_1 = \Theta_{1,j}$ to simplify our graphical illustration.) The result is that for the j-th fiber product, we consider systems of the form

$$g_j(\phi_j; p) = \begin{Bmatrix} e^{i\Theta_{1,j}} + \ell_2\theta_{2,j} - (x + iy) \\ e^{-i\Theta_{1,j}} + \ell_2\bar{\theta}_{2,j} - (x - iy) \\ \theta_{2,j}\bar{\theta}_{2,j} - 1 \end{Bmatrix}, \tag{11}$$

where $\Theta_{1,j}$ is set equal to a random constant, and $\phi_j = (\theta_{2,j}, \bar{\theta}_{2,j})$, $p = (\ell_2, x, y)$. [We drop the polynomial $\theta_1\bar{\theta}_1 - 1$ present in (10), because it is always satisfied when we specify angle Θ_1 to form (11).] Then, to search for a self-motion with bi-dimension $(\mathfrak{b}, 1)$, we consider systems of the form

$$G_k^{(\mathfrak{b},1)} = \{g_1(\phi_1; p), \ldots, g_k(\phi_k; p), \mathcal{L}_\mathfrak{b}(p)\}. \tag{12}$$

7.1.1. Case $\ell_1 = \ell_2$

In this case, we set $\ell_2 = 1$, and parameter space is $(x, y) \in \mathbb{C}^2$. For general (x, y), $V(f)$ is two isolated points, that is, a vertical line through a general point (x, y) pierces the surface in two isolated points, as shown in Figure 5(a). As (x, y) vary, this sweeps out the 2-dimensional surface D_0 whose general points have mobility $\mathfrak{m} = 0$.

To search for self-motions of mobility $\mathfrak{m} = 1$, we consider $V(g_1)$. This is the slice of a horizontal plane through the surface of Figure 4(c), which gives a circle in (x, y) as Θ_2 turns, as illustrated in Figure 5(b). The case

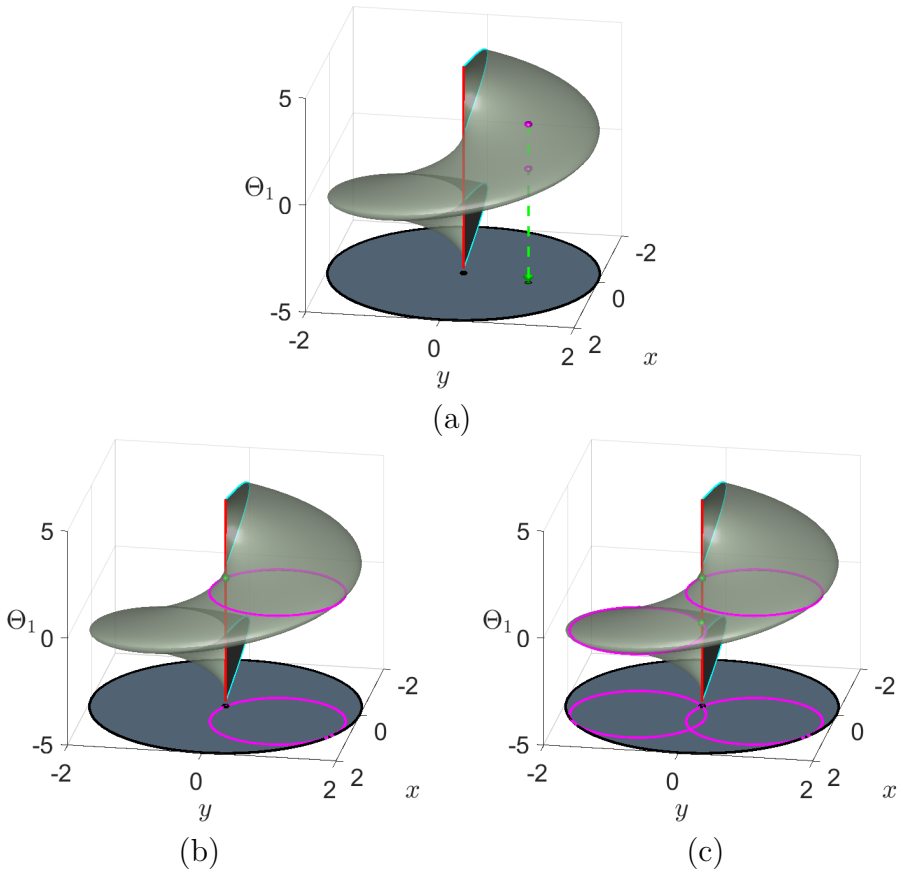

Figure 5: Slices of the 2R robot's solution manifold, case $\ell_2 = 1$.

$(\mathfrak{b}, \mathfrak{m}) = (1, 1)$ solves $V\big(G_1^{(1,1)}\big)$, which slices this circle with a vertical plane general in (x, y)-coordinates to get two points. When considered as solutions to $V(f)$ with (ℓ_2, x, y) held constant, one finds that these points are isolated in (Θ_1, Θ_2), that is, they do not have self-motion. Thus, we find that there is no self-motion of bi-dimension $(\mathfrak{b}, \mathfrak{m}) = (1, 1)$.

Proceeding to search for self-motions of bi-dimension $(\mathfrak{b}, \mathfrak{m}) = (0, 1)$, we solve $V(G_2^{(0,1)})$. This has no slices in parameter space; instead, it intersects the projections of two circles in the base coordinates to get two isolated points, as shown in Figure 5(c). One of these has mobility 0, while the one with $(x, y) = (0, 0)$ has mobility 1. This is the self-motion, set D_1 with bi-dimension $(\mathfrak{b}, \mathfrak{m}) = (0, 1)$ embedded inside D_0.

Notice that $G_2^{(0,1)} = 0$ is a necessary condition for isolating witness points on a self-motion of bi-dimension $(\mathfrak{b}, \mathfrak{m}) = (0, 1)$, but it is not sufficient; we have to test the mobility of the sample points we obtain. Doing so, one of the sample points turns out to be a false solution point, meaning it has mobility 0, while the second point turns out to be a true self-motion.

7.1.2. Case general ℓ_2

In the previous case, we set $\ell_2 = 1$, knowing that this would give a self-motion. Now we consider letting ℓ_2 be general, and show that we can find the exceptional case where self-motion occurs. With a 3-dimensional parameter space, (ℓ_2, x, y), we cannot easily plot results, but we can report the outcome of computations.

Since system $G_k^{(\mathfrak{b},1)}$ has $3k + \mathfrak{b}$ equations in $2k + 3$ unknowns,

$$(\phi_1, \ldots, \phi_k; p) = \big((\theta_{2,j}, \bar{\theta}_{2,j}), j = 1, \ldots, k; \ell_2, x, y\big),$$

we need to consider $k \geq 3 - \mathfrak{b}$ to slice out isolated points on a set of bi-dimension $(\mathfrak{b}, \mathfrak{m}) = (\mathfrak{b}, 1)$. When solving system $G_k^{(\mathfrak{b},1)}$ using Bertini [33], we put each of $\theta_{2,j}$ and $\bar{\theta}_{2,j}$, $j = 1, \ldots, k$, in its own variable group and $\{\ell_2, x, y\}\}$ in another variable group. The resulting $(2k + 1)$-homogeneous homotopies solve the k-order fiber product with the fewest number of homotopy paths.

For $\mathfrak{b} = 2$, Bertini tracks 2 homotopy paths to find that $V\big(G_1^{(2,1)}\big)$ has 2 isolated points. Both have mobility 0, showing that there is no mobility 1 set with base dimension 2. For $\mathfrak{b} = 1$, system $G_2^{(1,1)}$ is solved by tracking 4 paths, again finding 2 isolated points with mobility 0. Finally, for $\mathfrak{b} = 0$, we solve $G_3^{(1,1)}$ by tracking 8 paths and obtain 2 isolated points. The projection of these points onto parameter space gives $(\ell_2, x, y) = (\pm 1, 0, 0)$, both of which

are mobility 1. We have found the self-motion condition: $\ell_2 = \pm\ell_1$. Of course, if we restrict length to be positive, only one of these counts, but our polynomial formulation of the problem could not account for an inequality, $\ell_2 > 0$.

7.2. A Seven-Link Mechanism

Figures 6(a,c) show a seven-link planar mechanism and a variable compliance device derived from it. The linkage has five passive R joints and two active slider inputs, q and s. For general (q, s), the linkage has only isolated roots, meaning that it assembles as a rigid structure. But as we know from the 2R robot analysis above, we expect that if links 1 and 4 have equal length, say $\ell_1 = \ell_4 = 1$, then for some settings of (q, s), the device will become one that has a self-motion. By adding the spring shown in Figure 6(c), the device becomes one that progressively transforms from very stiff to very soft as the linkage structure approaches a self-motion configuration. For this exercise, we will assume that links 2 and 3 have equal length ℓ and the sliders are located distance h above and below the ground pivot of link 1.

Although the device was designed knowing the self-motion characteristic of a 2R robot, it is illustrative to see how the fiber product reveals this. The two loop equations of the device can be written as

$$\tilde{f} = \begin{Bmatrix} e^{i\Theta_1} + \ell e^{i\Theta_2} + e^{i\Theta_4} - (q + ih) \\ e^{i\Theta_1} + \ell e^{i\Theta_3} + e^{i\Theta_4} - (s - ih) \end{Bmatrix}. \tag{13}$$

These equations can be converted to a polynomial system in a similar manner as we used to convert the 2R robot loop equation in (9), from exponential form to polynomial form in (10). For brevity, we do not write out the details. With ℓ and h given and Θ_1 set to a constant slicing value, the resulting system has 7 equations in 8 unknowns, $(\phi; p) = (\theta_2, \bar{\theta}_2, \theta_3, \bar{\theta}_3, \theta_4, \bar{\theta}_4; q, s)$. The 7 equations come from $\tilde{f}$ and its conjugate plus 3 unit length conditions $\theta_j\bar{\theta}_j - 1$, $j = 2, 3, 4$.

Figure 6(b) shows the four assembly configurations of the device for general (q, s). As (q, s) vary over $\mathbb{R}^2$, these four solutions sweep out a 4-sheeted surface of $(\Theta_1, \Theta_2, \Theta_3, \Theta_4)$ versus (q, s). Figure 7(a) shows this surface in 3D by projecting it to $\cos\Theta_1$ versus (q, s). This is the mobility 0 surface D_0. Embedded inside D_0 is D_1, consisting of four self-motions, which appear as red vertical lines in Figure 7(a).

We can find the mobility 1 self-motions by slicing D_0 at two general values of Θ_1, and intersecting the projections of these two curves in the (x, y)-plane.

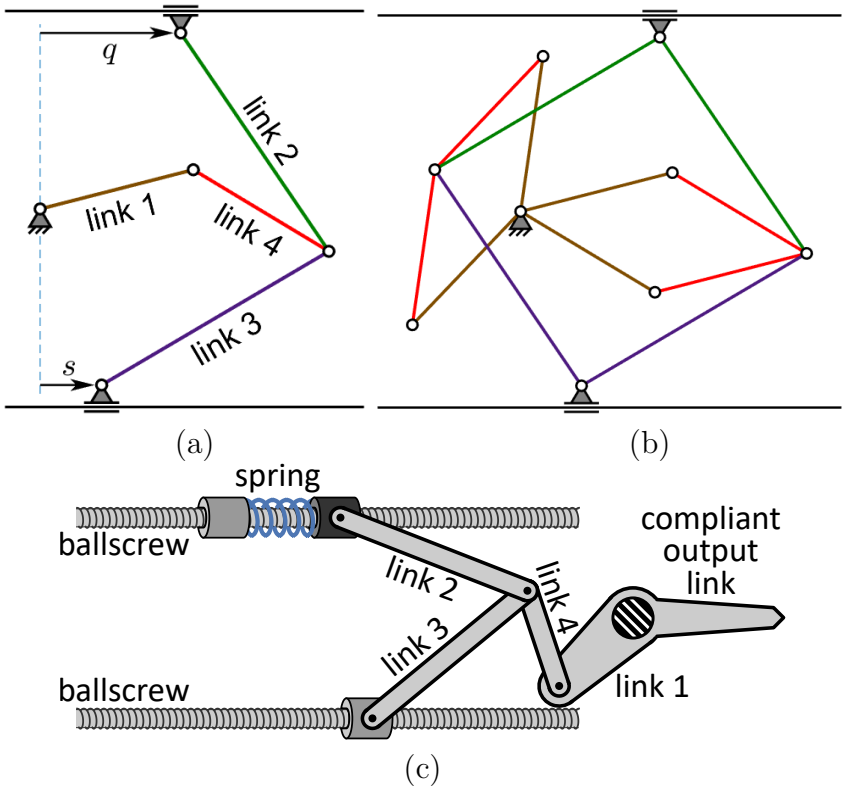

Figure 6: A seven-link mechanism: (a) kinematic sketch with two slider inputs, (b) four assembly configurations for general (q, s), (c) a derivative device with variable compliance.

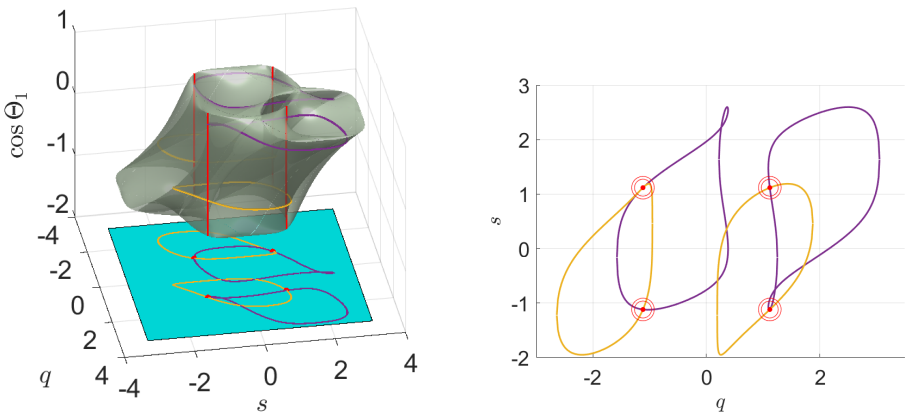

Figure 7: (a) Seven-link surface, D_0, with embedded curves, D_1, and (b) revealing self-motions D_1 by intersecting projections of slices of D_0.

Figure 7(b) shows this projection by itself, with the four self-motion points highlighted. One may notice that there are additional intersections of the two curves that are points having mobility 0 instead of 1.

7.3. Gimbal Lock

Consider the serial spherical 3R gimbal, often used as the 3R wrist of a serial-link robot. For most orientations of the third link, there are two isolated solutions of the inverse kinematics problem. This means that D_0 is a set of bi-dimension $(3, 0)$. Gimbal lock occurs when the wrist has a self-motion while the orientation of the third link remains stationary.

We may formulate kinematic equations starting from a reference configuration with axis 1 aligned with $\hat{x} = [1, 0, 0]$, axis 2 aligned with $\hat{y} = [0, 1, 0]$, and axis 3 aligned with $\hat{z} = [0, 0, 1]$. Defining $[\mathcal{R}(s, \phi)]$ as a rotation matrix about axis s and by angle ϕ, the orientation of the last link is

$$[\mathcal{R}(\hat{x}, \phi)][\mathcal{R}(\hat{y}, \psi)][\mathcal{R}(\hat{z}, \theta)] = [\mathcal{Q}], \tag{14}$$

$$[\mathcal{Q}] = \begin{bmatrix} q_0^2 + q_1^2 - q_2^2 - q_3^2 & 2(q_1q_2 - q_0q_3) & 2(q_1q_3 + q_0q_2) \\ 2(q_1q_2 + q_0q_3) & q_0^2 - q_1^2 + q_2^2 - q_3^2 & 2(q_2q_3 - q_0q_1) \\ 2(q_1q_3 - q_0q_2) & 2(q_2q_3 + q_0q_1) & q_0^2 - q_1^2 - q_2^2 + q_3^2 \end{bmatrix}, \tag{15}$$

$$g(q) = q_0^2 + q_1^2 + q_2^2 + q_3^2 - 1 = 0, \tag{16}$$

where (ϕ, ψ, θ) are X–Y–Z Euler angles, and $q = (q_0, q_1, q_2, q_3)$ is a unit

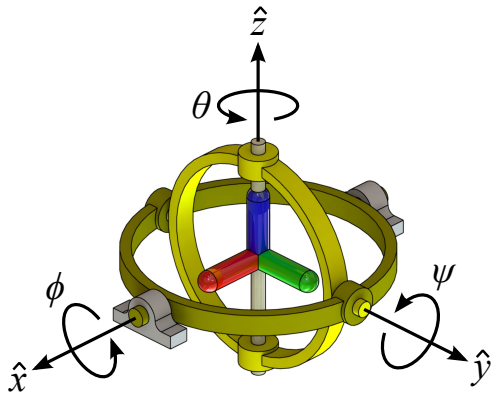

Figure 8: A spherical gimbal

quaternion representation of orientation. We wish to find the exceptional set where the Euler angles move while the quaternion is held constant.

As a first step, we eliminate θ from (14) by multiplying both sides by $\hat{z}$:

$$[\mathcal{R}(\hat{x},\phi)][\mathcal{R}(\hat{y},\psi)]\hat{z} = [\mathcal{Q}]\hat{z},$$

which with (15) and the substitutions $c_\phi = \cos\phi$, $s_\phi = \sin\phi$, $c_\psi = \cos\psi$, $s_\psi = \sin\psi$ expands to the system

$$f(x;q) = \left\{ \begin{bmatrix} s_\psi \\ -s_\phi c_\psi \\ c_\phi\, c_\psi \end{bmatrix} - \begin{bmatrix} 2(q_1q_3 + q_0q_2) \\ 2(q_2q_3 - q_0q_1) \\ q_0^2 - q_1^2 - q_2^2 + q_3^2 \end{bmatrix} \right\} = 0, \qquad (17)$$
$$\begin{matrix} {c_\phi}^2 + {s_\phi}^2 - 1 \\ {c_\psi}^2 + {s_\psi}^2 - 1 \end{matrix}$$

where $x = (c_\phi, s_\phi, c_\psi, s_\psi)$. We require the quaternion q to be unit length, so the system of interest is $\{f(x;q), g(q)\}$.

For a general unit quaternion $q^* \in V(g)$, $V(f(\phi,\psi;q^*))$ is a pair of non-singular points, so D_0 is bi-dimension $(3,0)$. An irreducible decomposition shows that there are no other 3-dimensional components in $V(f,g)$. This implies that any exceptional sets must be embedded inside D_0 and can be no more than 2-dimensional. To search for gimbal lock configurations, where mobility is 1, we start by checking for sets of bi-dimension $(1,1)$. Accordingly, the system to solve is

$$G_2^{(1,1)}\{f(x_1;q), \mathcal{L}_1(x_1), f(x_2;q), \mathcal{L}_1(x_2), g(q), \mathcal{L}_1(q)\}. \qquad (18)$$

This is a system of 14 polynomials in 12 variables, nevertheless it is self-consistent and has 32 isolated solutions, all nonsingular. Checking the rank of the Jacobian matrix at each of these shows that 16 have zero-dimensional fibers, meaning that they are not samples on self-motion curves. The remaining 16 split into two groups of 8 solutions, as follows:

$$\begin{array}{lllll} \text{Type 1}: & c_{\psi_1} = c_{\psi_2} = 0, & s_{\psi_1} = s_{\psi_2} = 1, & q_0 = q_2, & q_1 = q_3. \\ \text{Type 2}: & c_{\psi_1} = c_{\psi_2} = 0, & s_{\psi_1} = s_{\psi_2} = -1, & q_0 = -q_2, & q_1 = -q_3. \end{array}$$

These correspond to the known gimbal lock configurations where $\psi = \pm 90°$. The 8 solutions in each type are distinct, as they have different values for ϕ and the quaternion q. The values obtained are determined by the slicing linears, so these will change if one chooses different coefficients in $\mathcal{L}_1(x_1)$, $\mathcal{L}_1(x_2)$, or $\mathcal{L}_1(q)$, but the conditions defining the two types of solutions will persist.

The interpretation of the two types of solutions is clear. Each places two conditions on q, resulting in a 1-dimensional set of orientations in the base. These are the orientations where the third joint axis of the gimbal is either parallel or antiparallel to the first. For each such orientation, there is a solution set of mobility 1 for (ϕ, ψ, θ) wherein ψ stays fixed at $\pm 90°$ while ϕ and θ rotate in opposite directions to keep the final orientation constant. Accordingly, these two sets each have bi-dimension $(\mathfrak{b}, \mathfrak{m}) = (1, 1)$.

Note that in this example, we sliced configuration space using general linears instead of setting an angle to a general value, as we did in the previous examples. If we had chosen to slice configuration space by picking general values of ϕ, we would find the same results using fewer solution paths. However, note that if we had tried to look for exceptions by choosing general values of ψ instead, we would miss the exceptions, which only happen at $\psi = \pm 90°$. This demonstrates that if one chooses to simplify by slicing in a subset of the joint variables instead of using general slices, then one must take care to make sure that all the cases of interest move with the targeted mobility in that subspace.

7.4. A Subfamily of 6R Loops

Finally, we consider a spatial example. Consider the subfamily of spatial 6R loops wherein all link offsets are zero and the links alternate between two geometries. That is, the odd links have length L_1 and twist angle α_1, while the even links have length L_2 and twist angle α_2. For treatments of

mobility for general 6R loops, see [12, 38] and their references. We present our treatment of this more limited subfamily as an illustration of how more advanced techniques from numerical algebraic geometry, in this case, the diagonal intersection algorithm, can help address harder problems than we have presented so far.

Excluding cases where successive joint axes are parallel, so that $\sin\alpha_1 \neq 0$ and $\sin\alpha_2 \neq 0$, we can model the mechanism using as variables the unit vectors along the joint axes [39]:

$$\mathbf{z}_1 = [0, 0, 1], \quad \mathbf{z}_6 = [0, -\sin\alpha_2, \cos\alpha_2], \tag{19}$$

$$\mathbf{z}_i \cdot \mathbf{z}_i = 1, \quad i = 2, 3, 4, 5, \tag{20}$$

$$\mathbf{z}_i \cdot \mathbf{z}_{i+1} = \cos\alpha_1, \quad i = 1, 3, 5, \tag{21}$$

$$\mathbf{z}_i \cdot \mathbf{z}_{i+1} = \cos\alpha_2, \quad i = 2, 4, \tag{22}$$

$$\sum_{i=1,3,5} \left(\frac{L_1}{\sin\alpha_1}\right) \mathbf{z}_i \times \mathbf{z}_{i+1} + \sum_{i=2,4,6} \left(\frac{L_2}{\sin\alpha_2}\right) \mathbf{z}_i \times \mathbf{z}_{i+1} = 0. \tag{23}$$

The last of these is a sum of position vectors around the loop, so it corresponds to 3 scalar equations. When the link parameters are given, $\mathbf{z}_1$ and $\mathbf{z}_6$ are determined by (19), and the remaining equations are a system of 12 equations in 12 variables, these being the 3 entries in each of the joint vectors $\mathbf{z}_2, \mathbf{z}_3, \mathbf{z}_4, \mathbf{z}_5$. One may confirm that for general parameters $L_1, \alpha_1, L_2, \alpha_2$, there are 16 nonsingular solutions, the same as for a completely general 6R loop. We aim to find exceptional members of this subfamily having mobility 1.

Suppose that there exists a mobility 1 exceptional set for general values of α_2. Then, picking a random value of α_2, $\mathbf{z}_1$ and $\mathbf{z}_6$ are determined by (19), and we study the solution set of (20–23). To proceed, it helps to rewrite (23) as

$$\sum_{i=1,3,5} r\mathbf{z}_i \times \mathbf{z}_{i+1} + \sum_{i=2,4,6} \sin\alpha_1 \mathbf{z}_i \times \mathbf{z}_{i+1} = 0, \qquad r = \frac{L_1 \sin\alpha_2}{L_2} \tag{24}$$

Finally, to make the system polynomial, we may make the substitutions $c_{\alpha_1} = \cos\alpha_1$ and $s_{\alpha_1} = \sin\alpha_1$ and append the trigonometric identity

$$g(c_{\alpha_1}, s_{\alpha_1}) = c_{\alpha_1}^2 + s_{\alpha_1}^2 - 1 = 0. \tag{25}$$

For brevity, we do not rewrite the system.

The motion variables are $x = (\mathbf{z}_2, \mathbf{z}_3, \mathbf{z}_4, \mathbf{z}_5) \in \mathbb{C}^{12}$ and the parameters are $p = (r, c_{\alpha_1}, s_{\alpha_1})$. The system $f(x;p)$ consists of 12 equations (20–22,24), and p is restricted to the unit circle condition (25), i.e., $p \in V(g) \subset \mathbb{C}^3$. The set of immobile loops, D_0, has bi-dimension $(2,0)$, and we wish to search for loops with mobility 1, i.e., D_1.

Let us begin by checking whether D_1 has any components with bi-dimension $(1,1)$. Such a set cannot be embedded inside D_0, because the total dimensions are the same, but it might exist as a separate component. To check, we could solve

$$G_1^{(1,1)} = \{f(x;p), \mathcal{L}_1(x), g(p), \mathcal{L}_1(p)\} \tag{26}$$

which is a system of 15 polynomials in 15 unknowns. However, we may simplify by using the observation that we are only interested in motions where all joints must move, because if any one of them is constant, the result is essentially a 5R mechanism. Accordingly, rather than taking a general linear slice, $\mathcal{L}_1(x)$, we slice in the motion variables by specifying a random value for the first joint angle, θ_1, and evaluate $\mathbf{z}_2$ using the equation

$$\mathbf{z}_2 = [\sin\theta_1 s_{\alpha_1}, -\cos(\theta_1) s_{\alpha_1}, c_{\alpha_1}]. \tag{27}$$

This automatically satisfies one equation in each of (20) and (21). Accordingly, we may drop those two equations from f, to get a new system that we still call $G_1^{(1,1)}$ with variables re-cast as $x = (\theta_1, \mathbf{z}_3, \mathbf{z}_4, \mathbf{z}_5) \in \mathbb{C}^{10}$:

$$G_1^{(1,1)}(x;p) = \{f(x;p), g(p), \theta_1 - s_1, \mathcal{L}_1(p)\}, \tag{28}$$

where s_1 is a random value. This system of 12 polynomials in 12 variables has total degree $2^7 3^3 = 3456$, but a 3-homogenous formulation reduces the number of paths to track to 992. Solving this system gives 56 nonsingular solutions, and 4 singular ones. The singular ones have $s_{\alpha_1} = 0$; these extraneous roots are the result of clearing s_{α_1} from the denominator in going from (23) to (24). For the nonsingular roots, a check of the rank of the Jacobian matrix shows that they all have zero mobility. Thus, there are no solution sets of bi-dimension $(1,1)$.

To find exceptional sets of bi-dimension $(0,1)$, one solves

$$G_2^{(0,1)} = \{f(x_1;p), \theta_{1,1} - s_1, f(x_2;p), \theta_{1,2} - s_2, g(p)\}, \tag{29}$$

where both s_1 and s_2 are random values, and $\theta_{1,1}, \theta_{1,2}$ are the instances of θ_1 in the two copies of f, respectively. Stacking up two copies of f to form

this fiber product significantly increases the number of paths to track. The total degree of this system is $2(2^6 3^3)^2 = 5,971,968$. As this is rather large, rather than solving it all at once, we can use a more advanced method, called *diagonal homotopy* [40]. The solutions $V\left(G_1^{(1,1)}\right)$ are a pseudo-witness set for the projection onto P of $V(\{f(x,\theta_1;p),\theta_1 - s_1, g(p)\})$ [41], so the intersection of two such projections can be computed by moving their slicing linears appropriately, as follows.

1. Let S_1 be the 56 nonsingular solutions of $V(G_1^{(1,1)})$, previously computed.
2. Track the paths starting at $(x;p) \in S_1$ in the homotopy

$$G_1^{(1,1)}(x;p) = 0, \quad \theta_1 = ts_1 + (1-t)s_2$$

   as t goes from 1 to 0. This produces S_2, a set of 56 nonsingular solutions with $\theta_1 = s_2$.
3. Let $S_{1\times 2}$ be the set $S_1 \times S_2$ consisting of the 56^2 points

$$S_{1\times 2} = \{(x_1,p_1,x_2,p_2) \mid (x_1,p_1) \in S_1, (x_2,p_2) \in S_2\}.$$

4. Track the paths starting at $S_{1\times 2}$ for the homotopy

$$h(x_1,p_1,x_2,p_2,t) = \begin{Bmatrix} f(x_1;p_1),\theta_{1,1} - s_1, g(p_1) \\ f(x_2;p_2),\theta_{1,2} - s_2, g(p_2) \\ t\mathcal{L}_1^{(1)}(p_1) + (1-t)(r_1 - r_2) \\ t\mathcal{L}_1^{(2)}(p_2) + (1-t)(c_{\alpha_{1,1}} - c_{\alpha_{1,2}}) \end{Bmatrix},$$

   as t goes from 1 to 0. Here, $\mathcal{L}_1^{(1)}(p)$ and $\mathcal{L}_1^{(2)}(p)$ are the slicing linears that were used in solving the two instances of $G_1^{(1,1)}$.

At the completion of Step 4, we have forced $r_1 = r_2$ and $c_{\alpha_{1,1}} = c_{\alpha_{1,2}}$. Due to the presence of $g(p_1)$ and $g(p_2)$ in the homotopy, this also forces $s_{\alpha_{1,1}} = \pm s_{\alpha_{1,2}}$. The ones with $s_{\alpha_{1,1}} = s_{\alpha_{1,2}}$ are valid, and the others are discarded. This leaves 663 points in the intersection. A test of the rank of the Jacobian matrix reduces these to 184 that have mobility 1. These are witness points for the components of D_1.

A full analysis of the 184 points is out of scope for this article. Suffice it to say that they appear in several symmetry groups. All the points in one of these groups has parameters that obey the relations $r = -s_{\alpha_1}$, $s_{\alpha_1} = -\sin\alpha_2$,

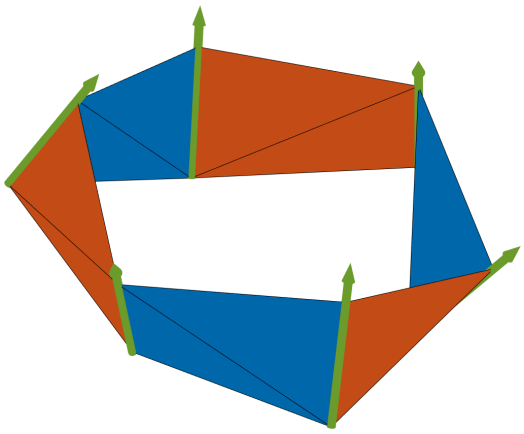

Figure 9: A spatial 6R closed-loop mechanism with mobility 1. Traveling clockwise around the loop, red links have positive twist α_2 and blue links have negative twist $\alpha_1 = -\alpha_2$.

which implies that $L_1 = L_2$. Hence, we have 6R linkages with mobility 1 in which all the link lengths are equal, all the joint offsets are zero, and the twist angles of the odd links are the negatives of the twist angles of the even links. In the terminology of [42], this is a "Bennett-based" 6R overconstrained mechanism. Figure 9 shows one such linkage in one of its assembly configurations.

8. Complex vs. Real

Although in applications only real joint angles and link parameters are meaningful, when solving polynomial systems, it is convenient to allow the variables to take complex number values. Since $\mathbb{C}$ is algebraically closed, this allows us to bring the full power of algebraic geometry to bear. However, this move comes with a caveat concerning the dimension of the sets we compute.

In all the examples presented in this paper, the dimensions of an algebraic set in complex space and its dimension as a set in real space are the same. This is because in algebraic geometry, we define dimension in both cases by the number of independent coordinates required to specify a local patch of the set. Since each complex coordinate has a real and an imaginary part, an n-dimensional algebraic set in complex space, say $A \subset \mathbb{C}^m$, $m \geq n$, is $2n$-real-dimensional. Ordinarily, if its subset of real points, $A \cap \mathbb{R}^m$, is not empty, that subset forms an n-real-dimensional set. The caveat is that the dimension of the set of real points could be smaller than n if their multiplicity

is higher. This is the borderline case where A touches $\mathbb{R}^m$ tangentially.

An illustrative example is $V(x^2+y^2-a) \subset \mathbb{C}^2$. In complex space, this is always a one-dimensional curve. For $a > 0$, its real part is also one-dimensional, a circle. For $a < 0$, the real part is empty. For the borderline case of $a = 0$, the complex curve factors into two lines, $V(x+iy)$ and $V(x-iy)$. These touch the reals at just the point $(x, y) = (0, 0)$, so the real part is zero-dimensional. But while general points of $V(x^2+y^2) \subset \mathbb{C}^2$ are nonsingular, the real point $(0, 0)$ lies at the intersection of the two lines and is singular with multiplicity 2.

This phenomenon has two implications for our method of searching for sets of exceptional mobility. First, after finding a mobility $\mathfrak{m} \geq 1$ set in complex space, one should check whether it contains real points or if instead the real subset is empty. Second, to find all sets with real mobility, say $\mathfrak{m}_{\Re}$, it may be necessary to consider complex sets with mobility $\mathfrak{m} \geq \mathfrak{m}_{\Re}$. When real mobility is lower than complex mobility, the real set is singular. The difference in mobility consists of extra infinitesimal "shaky" degrees of freedom. If such shakiness is not of interest, one can dispense with the extra work of searching for complex sets of mobility $\mathfrak{m} > \mathfrak{m}_{\Re}$.

9. Discussion and Future Work

We have discussed how mechanisms of exceptional mobility can be found by solving fiber product systems using numerical algebraic geometry, and shown this in action on planar, spherical and spatial cases. Geometrically, to hunt for mechanisms of mobility $\mathfrak{m}$, we slice the motion variables with $\mathfrak{m}$ independent linear equations and project that slice onto the parameter space. If a subfamily of mobility $\mathfrak{m}$ exists, it will lie somewhere in the projection. Repeating this gives multiple projections that all contain the sought-after subfamily, which is then revealed by intersecting the projections.

It is simple to formulate the fiber product systems as multiple copies of the loop equations along with extra linear equations that perform the slicing. After forming such a system, one may apply a program like Bertini to solve the resulting polynomial system using numerical homotopy methods.

The naive approach of stacking up multiple copies of a polynomial system gives a fiber product system with a total degree that grows exponentially. Without further innovations, this rapid growth is a barrier to computing exceptional sets for complex mechanisms. However, as our treatment of a

subfamily of 6R spatial loops illustrates, the naive approach can be improved upon by using the diagonal homotopy technique.

In the examples presented herein, we did not consider any cases where a fiber product beyond order 2 was required. Deeper exploration into larger parameter spaces will require the development of algorithms customized specifically for solving higher-order fiber products. The key to progress will likely hinge on taking advantage of symmetries, noting, for example, that if $(x_1, x_2; p)$ is a point in the solution set of a second fiber product system, then so is $(x_2, x_1; p)$. In higher-order fiber products, the full symmetry group of all permutations holds. The exploitation of symmetry is planned for future work. Meanwhile, the technique already has promise for finding mechanisms of exceptional mobility that are not embedded too deeply in their parameter spaces.

The purpose of this article has been to lay the groundwork for future endeavors by showing how mechanisms of exceptional mobility can be formulated using concepts from algebraic geometry, and in particular, how a fiber product formulation can help expose sets of exceptional mobility that are embedded inside sets of lower mobility.

References

[1] A. J. Sommese, C. W. Wampler, Exceptional sets and fiber products, Foundations of Computational Mathematics 8 (2008) 171–196.

[2] G. T. Bennett, A new mechanism, Engineering 76 (1903) 777.

[3] J. M. Hervé, Analyse structurelle des mécanismes par groupe des déplacements, Mechanism and Machine Theory 13 (1978) 437–450.

[4] G. Gogu, Mobility of mechanisms: a critical review, Mechanism and Machine Theory 40 (2005) 1068–1097.

[5] E. Delassus, Les chaînes articulées fermées et déformables à quatre membres, Bull. Sci. Math 46 (1922) 283–304.

[6] K. Waldron, A study of overconstrained linkage geometry by solution of closure equations—Part II. Four-bar linkages with lower pair joints other than screw joints, Mechanism and Machine Theory 8 (1973) 233–247.

[7] F. Myard, Contribution à la géométrie des systèmes articulés, Bulletin de la Société Mathématique de France 59 (1931) 183–210.

[8] M. Goldberg, New five-bar and six-bar linkages in three dimensions, Transactions of the American Society of Mechanical Engineers 65 (1943) 649–656.

[9] K. J. Waldron, Hybrid overconstrained linkages, Journal of Mechanisms 3 (1968) 73–78.

[10] J. E. Baker, The Bennett, Goldberg and Myard linkages—in perspective, Mechanism and Machine Theory 14 (1979) 239–253.

[11] C. Song, Y. Chen, I.-M. Chen, A 6R linkage reconfigurable between the line-symmetric Bricard linkage and the Bennett linkage, Mechanism and Machine Theory 70 (2013) 278–292.

[12] C. Mavroidis, B. Roth, Analysis and synthesis of overconstrained mechanism, in: International Design Engineering Technical Conferences and Computers and Information in Engineering Conference, volume 12846, American Society of Mechanical Engineers, 1994, pp. 115–133.

[13] A. Karger, Classification of 5R closed kinematic chains with self mobility, Mechanism and Machine Theory 33 (1998) 213–222.

[14] S. Roberts, On three bar motion in plane space, Proceedings London Mathematical Society s1-7 (1875) 14–23.

[15] E. A. Dijksman, Motion Geometry of Mechanisms, CUP Archive, 1976.

[16] S. N. Sherman, J. D. Hauenstein, C. W. Wampler, A general method for constructing planar cognate mechanisms, Journal of Mechanisms and Robotics 13 (2021) 031009.

[17] A. Karger, Self-motions of Stewart–Gough platforms, Computer Aided Geometric Design 25 (2008) 775–783.

[18] M. L. Husty, A. Karger, Self-motions of Griffis-Duffy type parallel manipulators, in: Proceedings 2000 ICRA. Millennium Conference. IEEE International Conference on Robotics and Automation. Symposia Proceedings (Cat. No. 00CH37065), volume 1, IEEE, 2000, pp. 7–12.

[19] G. Nawratil, Types of self-motions of planar Stewart Gough platforms, Meccanica 48 (2013) 1177–1190.

[20] J. D. Hauenstein, S. N. Sherman, C. W. Wampler, Exceptional Stewart–Gough platforms, Segre embeddings, and the special Euclidean group, SIAM Journal on Applied Algebra and Geometry 2 (2018) 179–205.

[21] K. Waldron, A study of overconstrained linkage geometry by solution of closure equations—Part 1. Method of study, Mechanism and Machine Theory 8 (1973) 95–104.

[22] A. Montes, M. Wibmer, Gröbner bases for polynomial systems with parameters, Journal of Symbolic Computation 45 (2010) 1391–1425.

[23] A. Montes, The Gröbner Cover, volume 27 of *Algorithms and Computation in Mathematics*, Springer, Cham, 2018.

[24] K. Arikawa, Kinematic analysis of mechanisms based on parametric polynomial system: Basic concept of a method using Gröbner cover and its application to planar mechanisms, Journal of Mechanisms and Robotics 11 (2019) 020906.

[25] R. H. Lewis, Dixon-EDF: the premier method for solution of parametric polynomial systems, in: Applications of Computer Algebra: Kalamata, Greece, July 20–23 2015, Springer, 2017, pp. 237–256.

[26] M. Pfurner, X. Kong, C. Huang, Complete kinematic analysis of single-loop multiple-mode 7-link mechanisms based on Bennett and overconstrained RPRP mechanisms, Mechanism and Machine Theory 73 (2014) 117–129.

[27] K. Wohlhart, Kinematotropic linkages, in: Recent Advances in Robot Kinematics, Springer, 1996, pp. 359–368.

[28] X. Kong, M. Pfurner, Type synthesis and reconfiguration analysis of a class of variable-dof single-loop mechanisms, Mechanism and Machine Theory 85 (2015) 116–128.

[29] X. Kong, Type synthesis of variable-dof single-loop spatial mechanisms using Bennett 4R mechanisms and Goldberg 5R mechanisms, Mechanism and Machine Theory 206 (2025) 105902.

[30] J. S. Dai, J. Rees Jones, Mobility in metamorphic mechanisms of foldable/erectable kinds, Journal of Mechanical Design 121 (1999) 375–382. doi:10.1115/1.2829470.

[31] B. H. Dayton, Z. Zeng, Computing the multiplicity structure in solving polynomial systems, in: Proceedings of the 2005 International Symposium on Symbolic and Algebraic Computation, ISSAC '05, Association for Computing Machinery, New York, NY, USA, 2005, p. 116–123.

[32] D. J. Bates, J. D. Hauenstein, A. J. Sommese, C. W. Wampler, Numerically solving polynomial systems with Bertini, volume 25 of *Software, Environments, and Tools*, Society for Industrial and Applied Mathematics (SIAM), Philadelphia, PA, 2013.

[33] D. J. Bates, J. D. Hauenstein, A. J. Sommese, C. W. Wampler, Bertini: Software for numerical algebraic geometry, 2006. URL: `bertini.nd.edu`.

[34] P. Breiding, S. Timme, Homotopycontinuation.jl: A package for homotopy continuation in Julia, in: Mathematical Software–ICMS 2018: 6th International Conference, South Bend, IN, USA, July 24-27, 2018, Proceedings 6, Springer, 2018, pp. 458–465.

[35] A. Leykin, Numerical algebraic geometry, Journal of Software for Algebra and Geometry 3 (2011) 5–10.

[36] J. Verschelde, Algorithm 795: PHCpack: A general-purpose solver for polynomial systems by homotopy continuation, ACM Transactions on Mathematical Software (TOMS) 25 (1999) 251–276.

[37] C. W. Wampler, Isotropic coordinates, circularity, and Bézout numbers: planar kinematics from a new perspective, in: International Design Engineering Technical Conferences and Computers and Information in Engineering Conference, volume 97577, American Society of Mechanical Engineers, 1996, p. V02AT02A073.

[38] Z. Li, J. Schicho, A technique for deriving equational conditions on the denavit–hartenberg parameters of 6r linkages that are necessary for movability, Mechanism and Machine Theory 94 (2015) 1–8.

[39] C. Wampler, A. Morgan, Solving the 6R inverse position problem using a generic-case solution methodology, Mechanism and Machine Theory 26 (1991) 91–106.

[40] A. J. Sommese, J. Verschelde, C. W. Wampler, Homotopies for intersecting solution components of polynomial systems, SIAM Journal on Numerical Analysis 42 (2004) 1552–1571.

[41] J. D. Hauenstein, A. J. Sommese, Witness sets of projections, Applied Mathematics and Computation 217 (2010) 3349–3354.

[42] J. E. Baker, A comparative survey of the Bennett-based, 6-revolute kinematic loops, Mechanism and Machine Theory 28 (1993) 83–96.